AIAA SciTech Forum
11–15 & 19–21 January 2021, VIRTUAL EVENT
AIAA Scitech 2021 Forum

10.2514/6.2021-1600

Design of a Virtual Wind Tunnel for CFD Visualization

David Paeres[1,*], Jean Santiago[1,†], Christian Lagares[1,‡], Wilson Rivera [2,§], Alan B. Craig [3,¶] and Guillermo Araya[1, ‖]
[1]*HPC and Visualization Lab, Dept. of Mechanical Eng., University of Puerto Rico at Mayaguez, PR 00681, USA.*
[2]*Dept. of Computer Science and Eng., University of Puerto Rico at Mayagüez, PR 00681, USA.*
[3]*University of Illinois, Urbana-Champaign, IL, USA.*

The widespread availability of high-performance commodity computing hardware has enabled technologies such as Virtual Reality and Augmented Reality to come out of research laboratories and enter the homes of many. Further, the widespread adoption of these technologies has caught the attention of the scientific community which is constantly researching potential applications. In the present study, we focus on applying virtual reality technologies as a scientific visualization tool. In particular, we show a virtual wind tunnel which enables the user to visualize complex and intricate turbulent flow patterns within an immersive environment. We also highlight potential research avenues within this particular area and present results for a sink flow DNS visualization.

I. Nomenclature

AR	=	Augmented Reality
VR	=	Virtual Reality
MR	=	Mixed Reality
UXF	=	Unity Experiment Framework
VWT	=	Virtual Wind Tunnel
GUI	=	Graphical User Interface
DNS	=	Direct Numerical Simulation
LES	=	Large Eddy Simulation
CFD	=	Computational Fluid Dynamics
TPC	=	Two-Point Correlation
FPG	=	Favorable Pressure Gradient
fps	=	Frames Per Second
ZPG	=	Zero Pressure Gradient
CFL	=	Courant-Friedrichs-Levy
FOV	=	Field Of View
ROI	=	Regions of Interest
HMD	=	Head Mounted Display

II. Introduction

The development of a Virtual Wind Tunnel (VWT) can undoubtedly appease the adage "See to believe." Virtual Reality (VR), Augmented Reality (AR), and Mixed Reality (MR) are technologies that attempt to blur the line between the physical world and a digital environment. Further, it provides a growing, virtually limitless, research environment which enables previously difficult or costly experiments. Such technologies are very useful for visual representation and excellent when dealing with complex structures that are hard to discern with the naked eye. As a motivating analogy, take the example of selling a car remotely and using Virtual Reality. As Flavian *et al.* [1] put forth, Mixed

*MSc Student and Research Assistant, AIAA Student Member
†Undergraduate Student and Research Assistant, AIAA Student Member
‡Doctoral Candidate and Research Assistant, AIAA Student Member
§Professor
¶Research Scientist
‖Associate Professor, AIAA Associate Fellow, araya@mailaps.org

Reality can significantly benefit the customer experience providing more dynamic and autonomous roles. To provide closure to the analogy, with such advanced technology, VR and other MR technologies enable a researcher to perform a scientific analysis of complex flows in complex geometries at a fraction of the effort and cost required in a physical setup.

The term "virtual wind tunnel" is not new. In fact, references to this goal can be dated back to 1991 [2]. The idea was refined and put forth again in 1993 by Bryson [3]. These early works were pioneering, but hindered by the technology of the time. The dramatic increase in computing capacity over the last 3 decades which can be attributed in part to the exponential growth in transistor count Moore's law [4] and exponential decrease in power consumption [5] has enabled near-real time visual effects impossible to implement with small-scale commodity hardware just three decades ago. To provide some context, Nvidia's GeForce 256 which was released circa 1999 contained close to 23 million transistors and was capable of 50 GFLOPs of computing performance with 128 MB of dedicated memory. Recently, Nvidia announced the Tesla A100 GPU which contains approximately 54.2 billion transistors and is capable of 19.5 TFLOPs of single-precision compute performance (312 TFLOPs of half precision performance for tensor operations) and provides 40 GB of dedicated high-bandwidth memory. This represents over 3 orders of magnitude increase in 20 years. This level of unprecedented compute performance opens new possibilities such as real-time, high-resolution interaction with a VWT without requiring a supercomputer to handle the millions of polygons required for rendering such applications.

To fully appreciate the VWT, it's required to be fully immersed in the Virtual Reality Environment; nonetheless we must first define the reality-virtuality continuum to provide a solid foundation for further discussion. Milgram and Kishino introduced the concept of a virtuality continuum nearly 25 years ago [6]. Milgram first advocated for the need of a taxonomy based on the concept of "Extent of World Knowledge" (the amount of information bleeding from the real environment into a virtual environment), "Reproduction Fidelity" (an attempt to quantify the image quality of the displays) and "Extent of Presence Metaphor" (a term to encapsulate the degree of immersion). Following a more modern approach, Flavian *et al.* [1] restate this taxonomy in 5 divisions. The first of these is the Real Environment; followed by the Augmented Reality were virtuality overlaps reality. The third is the Pure Mixed Reality where virtuality and reality are coalesced. The fourth is Augmented Virtuality where reality overlaps with virtuality. The last of these segments proposed by Flavian et. al. is the Virtual Environment. Perhaps the most difficult of these segments to acknowledge, which also helps to clarify the others divisions, is the Pure Mixed Reality located at the middle of the spectrum. Pure MR could be explained as the generation of virtual objects with an awareness of the real environment. Retaking our earlier analogy, imagine a virtual car where top, sides or bottom perspectives can be seen depending user's altitude and location; in other words, the virtual environment is "aware" of the user's physical environment.

The VWT proposed in the present work is directly linked to the benefits and limitations that current VR technology has, for example in education. Nor Farhah Saidin et al. [7] presented advantages and applications of AR in education. Their research studies suggest that lessons supported by technology leads to innovative forms of teaching and learning compared to traditional methods. They stated that governments should implement initiatives to improve the effectiveness of the teaching process. They also suggest AR provides an excellent opportunity especially for science subjects. The same study highlighted numerous other research studies conducted by many authors in different educational fields, for example **Table 1**, which is partially reproduced from Farhah et al. [7], concisely summarize some of these studies that agree on a similar conclusion: "The results of implementing AR provides a good feedback while motivating students to learn and remain engaged" [7].

Notwithstanding, these advantages are not without crucial limitations (as was alluded earlier). The same studies identified current limitations like internet latency/bandwidth; computers' memory capacity and physical speed limits (the speed of light is the ultimate limiting factor for latency); and the difficulties associated with software-interface troubleshooting for users. More recently, Jaziar Radianti et al. [8] reviewed how to optimize VR applications for educational purposes, especially at the higher education level. They stated that students are more likely to retain more information when using VR exercises and perform better when applying what had been learned. They acknowledged that the perceived degree of immersion in VR differs by individual. Further, there is still ambiguity and a lack of understanding of the equipment considered as immersive technology [8]. Consequently, one could argue that VR/AR technology needs to evolve by eliminating non-fully-immersive feeling. Roughly 2 decades ago, Lawrence Rosenblum [9] outlined a plausible path for this evolution. He outlined key areas the technologies researchers should focus their improvements to properly develop the futuristic technology, mentioning possibilities ranging from ultra-light weight haptic sensors to realistic interfaces to obtain a hard-to-distinguish environment (with respect to reality). Besides

improving sensors for better virtual environment perspectives, the hardware and software need to be fast [10] [11] and smooth enough without having data memory size constraints.

Table 1 Advantages of AR for Education (Partially reproduced from [7])

Author	Advantage of AR
Singal et al. [12]	Provides support for a more seamless interaction across the virtual reality continuum. Furthermore, it enables the integration of a tangible interface for object manipulation.
Coffin et al. [13]	Enables instructors to strengthen the understanding of students in a classroom by augmenting physical objects with virtual artifacts
Burton et al. [14]	It provides a decentralization of the formal classroom that empowers students to continue learning outside school limits.
Medina, Chen and Weghorst [15]	Enables the visualization of complex interactions such as those among amino acids and protein building as both static and dynamic 2D/3D images

Game engines platforms and VR technology can perfectly merge for scientific procedures. For example, Brookes et al.[16] performed a study of the human behavior with VR and using Unity Engine as platform. First, they describe a reference software called PyschToolBox which enables experiments to study the users' vision, this software was created in a way to be accessible for non programmers by including graphical user interface (GUI). Therefore, experimenters with no computer programming skills can conduct the examinations. Following the concept of PyschToolBox, the authors designed and proposed Unity Experiment Framework (UXF) for studying human behavior. UXF provides the necessary tools to create the experiments, with an optional GUI, allows the experimenter to easily: design the experiment's structure; define dependent variables and setting the independent ones, and editing display interface for the user's convenience. A useful feature of UXF is the cloud-based platform, where the experiments can be performed outside of a laboratory. The data collected by the software can go in and out to a server so the researchers can retrieve the data at far distances from where the experiment was conducted. To confirm the UXF reliability, the authors performed a study between adults and children to examine their visual response to a virtual swinging room. The results of the experiment were that children showed less postural stability than adults, as was expected from the previously research done by others in the past years [16].

The performed literature review has shown the applicability of VR and other technologies typically limited to the game industry to scientific endeavors. The motivation for the present work is that with currently available technologies which include sufficiently powerful GPUs, state-of-the-art game engines, a modern head-mounted VR display and sufficient pre-generated flow data a sufficiently realistic wind tunnel can be generated for immersive scientific visualization. In the present work, we plan to visualize the boundary layer separation over concave-convex walls with varying levels of complexity in terms of geometry. The necessary software foundations will be laid out to enable the rapid insertion of new flow fields. For future, the plan of this virtual wind tunnel is take the visualization abilities as advantages to model others different cases, regardless scenarios' geometries or CFD solver softwares. Further, we present preliminary results for a sink-flow DNS visualization. As part of the concluding remarks, we present future research avenues which coalesce with our research group's interests.

III. Numerical Methods

In recent decades, the area of Computational Fluid Dynamics (CFD) has been leveraging the significant growth of high-performance computational power for high-fidelity simulations as a means of predicting turbulent flow behavior and transport phenomena. The accurate understanding of the physics behind the effects of external conditions (i.e., streamwise pressure gradient, compressibility, wall curvature or Reynolds number dependency) on boundary layers and turbulent structures is crucial in the development of more efficient turbulence models. In addition, not only low/high order statistics computation of turbulent boundary layers is important but also the visualization of Two-Point Correlation (TPC) coherent structures and turbulent events contributes to the better knowledge of the flow because provide a simple, yet powerful, representation of correlated zones [17]. These zones are typically referred to as very-large scales of

motion (VLSM) which are responsible (in part) for the transport of thermal energy and other passive scalars such as contaminant, pollutant, humidity, etc.

IV. DNS Details

Direct Numerical Simulation (DNS) is a numerical tool that resolves all turbulence length and time scales; thus, it provides high spatial/temporal resolution flow data within a computational domain. Moreover, turbulent boundary layers that evolve along the flow direction are ubiquitous and show a non-homogeneous condition along the streamwise direction due to turbulent entrainment.

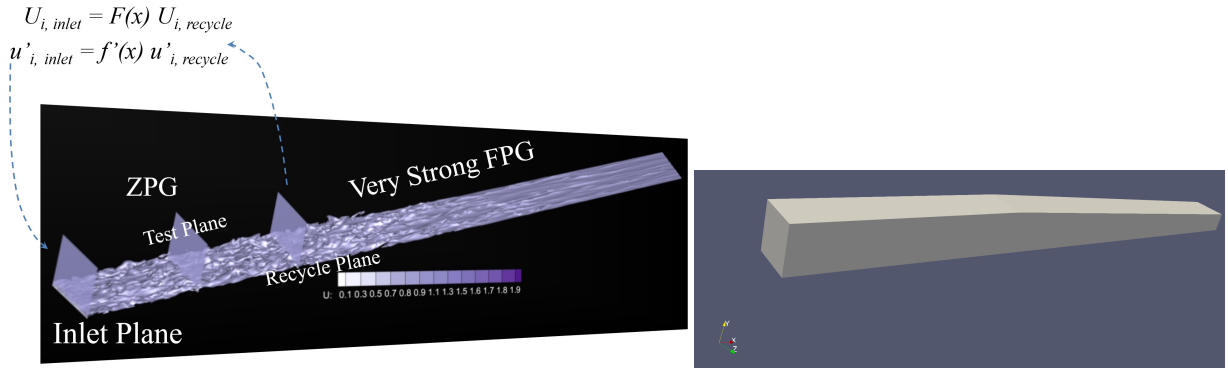

Fig. 1 (a) Schematic of the turbulent inflow generation methodology and (b) computational domain.

From a computational point of view, these types of boundary layers (i.e., spatially-developing boundary layers) possess enormous numerical challenges, due to the need for accurate and time-dependent inflow turbulence information. Moreover, accounting for the effects of Favorable Pressure Gradient (FPG) adds significant complexity to the problem, since the boundary layer is shrinking and characterized by smaller elongated turbulent coherent structures in the near wall region. We are making use of the Dynamic Multi-scale Approach ([18]), a method for prescribing realistic turbulent velocity inflow boundary conditions, later extended to thermal boundary layers in [19]. It is based on the rescaling-recycling method proposed by [20]. The principal idea of the rescaling-recycling method is to prescribe time-dependent turbulent information at the “inlet" plane based on the transformed flow solution downstream, from a plane called “recycle", by using scaling laws, as seen in Figure 1 (a). Furthermore, in our proposed new approach there is no need to use an empirical correlation (as in [20]) in order to compute the inlet friction velocity, such information is deduced dynamically by involving an additional plane, the so called test “plane" located between the inlet and recycle stations. Here, the friction velocity is defined as $u_\tau = \sqrt{\tau_w/\rho}$, where τ_w is the wall shear stress and ρ is the fluid density. Figure 1 (a) shows an iso-surface of instantaneous velocity in the computational domain of incompressible flow, consisting of a Zero Pressure Gradient (ZPG) region (or “precursor") to feed inflow turbulent information with an approximate length of $20\delta_{inlet}$ followed by a FPG region of length $40\delta_{inlet}$, where δ_{inlet} is the measured 99% boundary layer thickness at the inlet. The inlet, test and recycle planes are located in the ZPG region, immediately preceding the FPG region. Favorable pressure gradient is prescribed by a top converging surface (sink flow) with an acceleration parameter of $K = 4.0 \times 10^{-6}$ (see Fig. 1 (b)). The acceleration parameter is defined as $K = \frac{\nu}{U_\infty^2}\frac{dU_\infty}{dx}$, where U_∞ is the freestream velocity and ν is the fluid kinematic viscosity, [21]. At the wall, the classical no-slip condition is imposed for velocities. An isothermal condition is prescribed for the temperature field at the wall, regarded as a passive scalar. The lateral boundary conditions are handled via periodicity. Dimensions of the composite computational domain (L_x, L_y and L_z) are $60\delta_{inlet}$, $4.3\delta_{inlet}$ and $4.3\delta_{inlet}$ along the streamwise (x), wall-normal (y) and spanwise (z) directions, respectively. The mesh configuration is $600 \times 80 \times 80$, which represents the numbers of points along x, y and z directions, respectively. The mesh resolution is $\Delta x^+ = 15$, $\Delta y^+_{min} = 0.2$, $\Delta y^+_{max} = 13$ and $\Delta z^+ = 8$, where superscript + indicates wall units. The Courant-Friedrichs-Levy (CFL) parameter is approximately 0.24 during the simulation and the time step is fixed at $\Delta t^+ \approx 0.19$. The reader is referred to [22] for more details. The flow acceleration is so strong in the FPG region that the flow exhibits “quasi-laminarization" features, i.e. the boundary layer has some turbulence residual. This is attributed to the momentum extracted from the turbulent transport by the pressure gradient forces in the FPG

zone. Figure 2 depicts the volumetric rendering of the instantaneous streamwise velocity by means of the Paraview visualization tool. It can be clearly seen the attenuation of velocity fluctuations as the flow penetrates further into the FPG region. This DNS case is under study for virtual reality purposes and further details are discussed later in the manuscript.

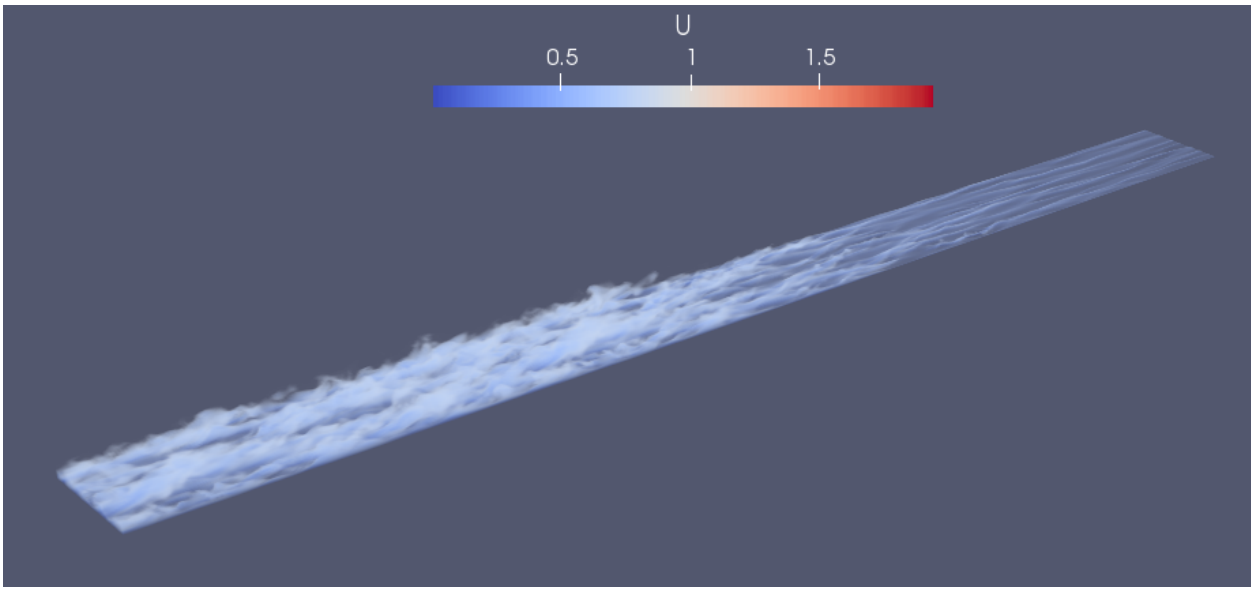

Fig. 2 Volumetric data rendering of the instantaneous streamwise velocity in the sink flow case.

V. Scientific Visualization

At the beginning, flow visualization by smoke and dye injection was the only technique available to describe coherent structures in turbulent flows [23], [24]. Generally speaking and based on the premise “seeing is believing", visualization techniques have substantially evolved in the last few decades spanning all disciplines [25]. According to Friendly [26], scientific visualization “is primarily concerned with the visualization of 3D+ phenomena (architectural, meteorological, medical, biological, etc.), where the emphasis is on realistic renderings of volumes, surfaces, illumination sources, and so forth, perhaps with a dynamic (time) component." Further suggested literature includes [27], [28] and [29]. In this regard, it is important to stress the relevance of identifying the target audience: the constituent parts, or formal attributes, of a visual product will change in relation to its purpose and intended audience. For example, a visualization for a scientific publication may incorporate very technical annotations, or use a color scale that fits a standard convention in a given field. On the contrary, a visualization intended as a dissemination product for stakeholders or the general public will not need as many technical details, or the color schemes would be chosen based on aesthetics rather than field conventions. In this project, we intend to create visual displays of CFD simulations oriented to: a) a scientific audience specialized in turbulence, and b) the general public as dissemination and outreach. For the first group, we are identifying and rendering relevant regions of interest (ROI) in the DNS database by means of standard scientific visualization software and custom visualizations tools.

Virtual reality (VR) applications fully immerse the user in a 3D virtual world, Craig & W. Sherman [30]. The procedure to create a virtual environment in CFD starts with the post-processing information from DNS data (ascii or binary format); this information is transformed via a Python code into a file structure understandable by the VR software (Unity-3D game engine), usually files with .obj extension (also experimenting with .usdz extension). Different properties of turbulent flows or iso-surfaces are visualized in the virtual environment. A workstation (see fig. 3 (a)) gathers the information of all input devices (e.g. controllers and base stations) to identify then which part of the numerical results are in the field of view (FOV) of the user and have to be rendered. To create a feeling of immersion and presence inside the virtual environment, the renders have to be recalculated to a speed of at least 30 frames per second (fps). Once the frames are rendered, they are sent to a head mounted display (HMD) which outputs a stereoscopic image in order to provide the user with the 3D illusion of depth. Fully immersed visualizations is performed on HTC Vive

VR kit. Figure 3 (b) shows a HTC Vive user in the early prototype VWT performing visualization of iso-surfaces of instantaneous streamwise velocity (about $0.8U_{\infty\ inlet}$, where $U_{\infty\ inlet}$ is the inlet freestream velocity) extracted from the DNS database. Approximately 600 frames were arranged and organized to create a fluid motion sensation. The entire video of this prototype virtual environment can be watched at `https://youtu.be/M6MGwgdvVkY`. The most recent version of the VWT has a more realistic environment appearance and also includes the virtual Gallery of Coherent Structures. Readers are encouraged to explore the latest VWT and the new in-house smartphone app FlowVisXR at DOI: `https://doi.org/10.1103/APS.DFD.2020.GFM.V0045`.

(a) (b)

Fig. 3 (a) HTC Vive VR kit, (b) student performing virtual flow visualization.

VI. Preliminary Results and Discussion

A. Sink Flow

In this section, we show and discuss results obtained in an early iteration of the proposed VWT. The results were obtained from a direct numerical simulation of an incompressible sink flow. Figures 4(a) and 4(b) show the instantaneous streamwise velocity at an upstream and downstream location respectively. The quasi-laminar region downstream can be clearly seen as was mentioned earlier, the VWT provides additional flexibility to "navigate" the flow field and identify events such as bulges, valleys and low/high speed streaks.

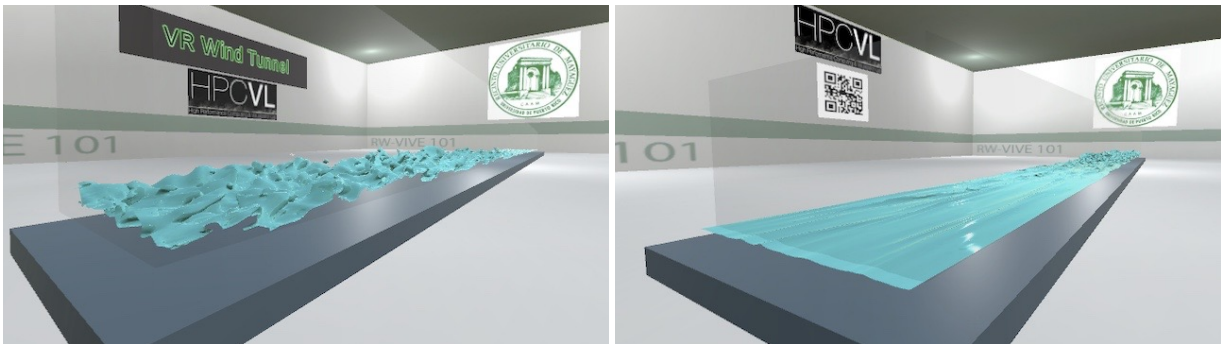

(a) (b)

Fig. 4 (a) Upstream turbulent flow , (b) Downstream quasi-laminar flow.

We also present a visualization from the VWT of the streamwise velocity fluctuations further demonstrating the versatility of the VWT to highlight different aspects of a dataset as needed. The user can explore the live animation of the DNS flow field in real-time, potentially revealing interesting phenomena that were not previously detected by lower-order visualization methods.

B. Others results

Figure 5 show the latest appearance of the virtual wind tunnel. Meanwhile the Figures 6(a) and 6(b) show an examples of TPC coherent structures for incompressible flow placed in the virtual Gallery of Coherent Structures, streamwise velocity fluctuations at $y^+ = 15$ and $y^+ = 1$ respectively.

Fig. 5 Virtual Wind Tunnel (VWT) with more realistic environment.

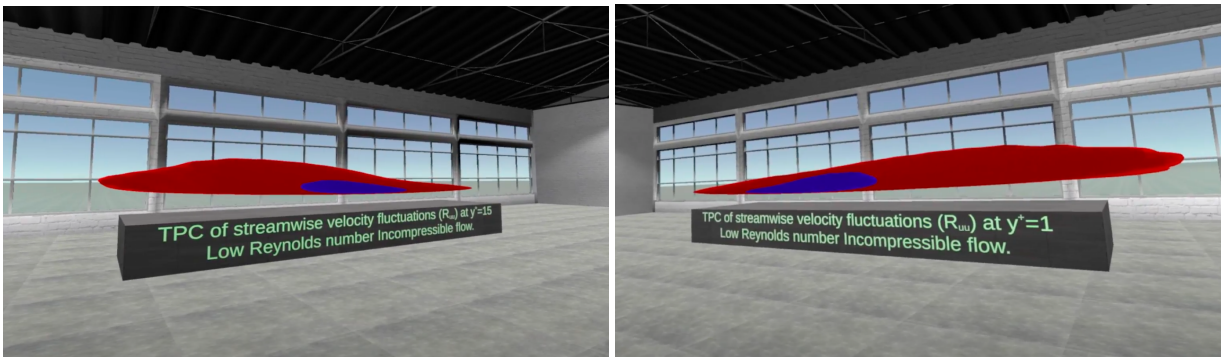

(a) (b)

Fig. 6 Streamwise velocity fluctuations at (a) $y^+ = 15$, (b) $y^+ = 1$.

C. Future Research Directions

The potential research directions enabled by this technology are quite numerous, but at the short term one could consider extending the capabilities of the current VWT to interact with a wider range of data formats thus enabling runtime loading of datasets regardless of software platform. A long term vision would enable near-real-time computing within the VWT, thus reducing storage requirements by allowing the GPU to compute fluctuations live, two-point-correlations, cross-correlations, and vary iso-surface levels without leaving the VWT environment. Perhaps an even more ambitious goal would be to establish a link between the VWT and a supercomputing resource enabling the VWT user to drive a simulation while visualizing the results in near-real-time.

VII. Conclusion

In summary, we present our proposed approach to enable a virtual wind tunnel. Following the discussed taxonomy, we argue for the use of mixed reality in scientific visualization and presented preliminary results for such endeavour. We also propose future research directions with the culminating goal of enabling near-real-time compute withing the VWT which would empower the user to perform rapid iteration and visualization without leaving the MR environment thus enhancing the extent of presence.

Acknowledgments

Christian Lagares acknowledges financial support from the National Science Foundation under grant no. 1906130. Guillermo Araya acknowledges subaward no. 074984-16663 (GECAT-University of Illinois), NSF-CAREER award no. 1847241 and AFOSR grant no. FA9550-17-1-0051. This work was supported in part by a grant from the DoD High-Performance Computing Modernization Program (HPCMP).

References

[1] Flavián, C., Ibáñez-Sánchez, S., and Orús, C., "The impact of virtual, augmented and mixed reality technologies on the customer experience," *Journal of Business Research*, Vol. 100, 2018, pp. 547–560.

[2] Bryson, S., and Levit, C., "The Virtual Windtunnel: An Environment for the Exploration of Three-Dimensional Unsteady Flows," Tech. rep., NASA Ames Research Center, 10 1991.

[3] Bryson, S., "The Virtual Windtunnel: Visualizing Modern CFD Datasets with a Virtual Environment," *IEEE Virtual Reality Annual International Symposium 1993*, IEEE Computer Society, 1993, pp. 390–395.

[4] Schaller, R. R., "Moore's law: past, present and future," *IEEE Spectrum*, Vol. 34, No. 6, 1997, pp. 52–59.

[5] Dennard, R. H., Gaensslen, F. H., Yu, H., Rideout, V. L., Bassous, E., and LeBlanc, A. R., "Design of ion-implanted MOSFET's with very small physical dimensions," *IEEE Journal of Solid-State Circuits*, Vol. 9, No. 5, 1974, pp. 256–268.

[6] Milgram, P., and Kishino, F., "A Taxonomy of Mixed Reality Visual Displays," *IEICE Transactions on Infromation System*, 1994.

[7] Saidin, N. F., Halim, N. D. A., and Yahaya, N., "A Review of Research on Augmented Reality in Education:Advanges and Applications," *International Education Studies*, Vol. 8, 2015.

[8] Radianti, J., an Jennifer Fromm, T. A. M., and Wohlgenannt, I., "A systematic review of immersive virtual reality applications for higher education: Design elements, lesson learned, and research agenda," *Computers Education*, Vol. 147, 2018.

[9] Rosenblum, L., "Virtual and Augmented Reality 2020," Vol. 20, 2000.

[10] Albert, R., Patney, A., Luebke, D., and Kim, J., "Latency Requirements for Foveated Rendering in Virtual Reality," *ACM Transactions on Applied Perception*, Vol. 14, No. 4, 2017.

[11] Elbamby, M. S., Perfecto, C., Bennis, M., and Doppler, K., "Toward Low-Latency and Ultra-Reliable Virtual Reality," *IEEE Network*, Vol. 32, No. 2, 2018, pp. 78–84.

[12] Singhal, S., Bagga, S., Goyal, P., and Saxena, V., "Augmented Chemistry: Interactive Education System," *International Journal of Computer Applications*, Vol. 49, 2012.

[13] Coffin, C., Bostandjiev, S., Ford, J., and Hollerer, T., "Enhancing Classroom and Distance Learning Through Augmented Reality," *Proceedings of EdMedia + Innovate Learning 2010*, edited by J. Herrington and C. Montgomerie, Association for the Advancement of Computing in Education (AACE), Toronto, Canada, 2010, pp. 1140–1147. URL `https://www.learntechlib.org/p/34777`.

[14] Peters-Burton, E., Frazier, W., Annetta, L., Lamb, R., Cheng, R., and Chmiel, M., "Modeling Augmented Reality Games with Preservice Elementary and Secondary Science Teachers," *Journal of Technology and Teacher Education*, 2011.

[15] Medina, E., Chen, Y.-C., and Weghorst, S., "Understanding Biochemistry with Augmented Reality," *Proceedings of World Conference on Educational Multimedia, Hypermedia and Telecommunications*, 2008.

[16] Brookes, J., Warburton, M., Algahdier, M., Mon-Williams, M., and Mushtaq, F., "Studying human behavior with virtual reality: The Unity Experiment Framework," *Behav Res*, Vol. 52, 2020, p. 455–463.

[17] Pope, S. B., *Turbulent Flows*, Cambridge University Press, 2000.

[18] Araya, G., Castillo, L., Meneveau, C., and Jansen, K., " A dynamic multi-scale approach for turbulent inflow boundary conditions in spatially evolving flows," *Journal of Fluid Mechanics*, Vol. 670, 2011, pp. 518–605.

[19] Araya, G., and Castillo, L., "DNS of turbulent thermal boundary layers up to $Re_\theta = 2300$," *Int. Journal of Heat and Mass Transfer*, Vol. 64, 2012, pp. 4003–4019.

[20] Lund, T., Wu, X., and Squires, K., "Generation of turbulent inflow data for spatially-developing boundary layer simulations," *Journal of Computational Physics*, Vol. 140, No. 2, 1998, pp. 233–258.

[21] Launder, B. E., "Laminarization of the turbulent boundary layer by acceleration," *Gas Turbine Lab., MIT., Cambridge*, Vol. Rept. No. 77, 1964.

[22] Araya, G., Castillo, C., and Hussain, F., "The log behaviour of the Reynolds shear stress in accelerating turbulent boundary layers," *Journal of Fluid Mechanics*, Vol. 775, 2015, pp. 189–200.

[23] Brown, G., and Roshko, A., "On density effects and large structure in turbulent mixing layer," *Journal of Fluid Mechanics*, Vol. 64, 1974, pp. 775–816.

[24] Winant, C. D., and Browand, F. K., "Vortex pairing : the mechanism of turbulent mixing-layer growth at moderate Reynolds number," *Journal of Fluid Mechanics*, Vol. 63, 1974, pp. 237–255.

[25] William R. Sherman, M. P. B., Alan B. Craig, and Bushell, C., "Scientific visualization," *Allen B. Jr. Tucker (Ed.), Chapter 35 of The Computer Science and Engineering Handbook. CRC Press, Boca Raton, FL.*, 1997.

[26] Friendly, M., "Milestones in the history of thematic cartography, statistical graphics, and data visualization," *York University, Department of Mathematics and Statistics*, 2009. URL `http://www.math.yorku.ca/SCS/Gallery/milestone/milestone.pdf`.

[27] Hansen, C. D., and Johnson, R., "The Visualization Handbook," *Elsevier*, 2005.

[28] Nielson, G. M., Hagen, H., and Muller, H., "Scientific Visualization: Overviews, Methodologies, and Techniques," *IEEE Computer Society*, 1997.

[29] McCormick, B. H., DeFanti, B., and Maxine, D., "Visualization in Scientific Computing," *ACM Press.*, 1987.

[30] Craig, A., Sherman, W., and Will, J., *Developing Virtual Reality Applications*, Morgan Kaufmann Publishing, 2009.